Spatial and temporal variability of greenhouse gas ebullition from temperate freshwater fish ponds

Carolin Waldemer[a,b], Matthias Koschorreck[a]

[a] Department of Lake Research, Helmholtz Centre for Environmental Research-UFZ, Brückstraße 3a, 39114 Magdeburg, Germany

[b] Corresponding author: Helmholtz Centre for Environmental Research-UFZ. E-mail address: carolin.waldemer@ufz.de

ABSTRACT

Fish ponds with their typically high carbon and nutrient inputs are relevant sources of greenhouse gases. However, not much is known about gas bubble emissions (ebullition) and their high spatiotemporal variability. This is the first study which quantified diffusive and ebullitive greenhouse gas emissions from temperate fish ponds. To improve greenhouse gas estimates, we investigated the diurnal and spatial variability of diffusive and ebullitive fluxes in 12 extensively to semi-intensively managed fish ponds near Bautzen, Germany. Emissions differed greatly between the different ponds but methane was consistently the predominant greenhouse gas. The feeding sites were hotspots with one order of magnitude higher ebullition rates compared to other parts of the ponds. At these hotspots, ebullitive fluxes of up to 38 L/m^{2}d were measured with a mean bubble methane content of 79 %, corresponding to a methane flux of 1.24 mol/m^{2}d. Methane accounted for 90% of the global warming potential in one fish pond but carbon dioxide emissions of up to 242 mmol/m^{2}d at the feeding sites were also significant. Nitrous oxide fluxes, in contrast, were low with 5 ± 9 µmol/m^{2}d. Greenhouse gas ebullition decreased exponentially along a transect from the feeding site into the pond and showed some diurnal fluctuations. While diffusion was higher during night, ebullition rates increased in the morning, presumably caused by higher benthivorous fish activity. Our results highlight the potential of temperate fish ponds as significant greenhouse gas sources and ebullition as a significant pathway. For robust quantification, both small scale spatial and temporal variability as well as the hotspot of the feeding area must be considered.

Keywords:

Ebullition, fish pond, aquaculture, methane (CH_4), greenhouse gas emissions

1. Introduction

Global climate change driven by elevated greenhouse gas (GHG) concentrations is one of the main challenges of our time. Understanding the interplay of GHG sources and sinks would enable us to give sound advice to politicians and decision-makers and make a change. Inland water bodies play a significant role in global GHG emissions (IPPC, 2021) but particularly high emissions were reported for aquaculture systems and fish ponds (Kosten et al., 2020; MacLeod et al., 2020; Rosentreter et al., 2021; Yuan et al., 2021). These ecosystems cover > 8 Mio ha globally and aquaculture production increases annually by 5 to 11% (FAO, 2018; Verdegem and Bosma, 2009). Significant quantities of carbon dioxide (CO_2), methane (CH_4) and nitrous oxide (N_2O) are emitted from fish ponds (Kosten et al., 2020; Yuan et al., 2019). Yuan et al (2019) estimated that the top 21 fish-producing countries emit 218 Tg CO_2-eq as CH_4 and 11 Tg CO_2-eq as N_2O from aquaculture annually, while Zhang et al. (2022) reported CH_4 emissions of up to 129 mmol/m^{2}d and 182 Tg CO_2-eq (CH_4 and CO_2) for Chinese aquaculture. Classical excavated earth ponds seem to play a large part in this (FAO, 2018; Yuan et al., 2019; Zhang et al., 2022).

The reason for the high potential of GHG emissions from aquaculture lies both in the morphology of the ponds and in the high loads of nutrients and organic carbon (OC), a combination of physical and biogeochemical properties. Unconsumed feed, fish feces, and nutrient stimulated aquatic primary production lead to a high availability of labile organic matter (OM) which fuels microbial mineralization and further promotes eutrophication and oxygen (O_2) depletion (Avnimelech and Ritvo, 2003; Kosten et al., 2020; Pechar, 2000; Yuan et al., 2019). Within 1 mm, anoxic conditions prevail in the sediment (Avnimelech and Ritvo, 2003). Due to the shallow water depth, sediment temperatures are high and drive microbial activity and methanogenesis once other external electron acceptors are depleted (Bastviken et al., 2004). Furthermore, the shallow and well-mixed nature of these ecosystems promotes GHG emissions through diffusion and ebullition, the flux via gas bubbles (e.g. Holgerson and Raymond, 2016). Bubbles form when the sum of the partial pressures of all dissolved gases exceeds the local total pressure, consisting of hydrostatic and atmospheric pressure

(Boehrer et al., 2021). Gaseous degradation products contribute to high dissolved gas pressures while the shallow water column leads to only a low counter pressure. Ebullition, however, shows a high small scale spatiotemporal variability and an episodic nature and is more relevant for the less soluble gases like CH_4 (Bastviken, 2009; Boehrer et al., 2021). Representative measurements require longer time periods and a sufficient number of sampling sites (Beaulieu et al., 2020; Kosten et al., 2020; Wik et al., 2016).

Due to the high spatiotemporal variability of ebullition, studies often focus on diffusive GHG fluxes and there are only a handful of aquaculture studies which investigate both gas transport pathways. With the exception of one study in Brazil (Flickinger et al., 2020), the vast majority of research to aquaculture was conducted in southeast Asia. But management practices, environmental conditions and aquaculture products vary greatly, and so do the reported GHG fluxes: From tanks to excavated ponds, from mixed species to monocultures with different biomass densities (fish, crab, shrimp etc.), from grain to artificial feed (several times a day to weekly at one feeding site or over the whole system), with additional aeration or fertilization, end of season drainage, dredging or liming – aquaculture strategies are manifold and GHG emissions estimates from aquaculture systems remain poorly constrained (Kosten et al., 2020; Yuan et al., 2019). For Chinese aquaculture, wide ranges of -0.03 to 565 g CH_4-C /m^2 yr and -382 to 551 g CO_2-C /m^2 yr and a strong emphasis on ebullition accounting for 70 to 99% of the total CH_4 emissions were reported (Zhang et al., 2022). But for other types of aquaculture management and for other regions systematic data are still completely lacking. So far, to our knowledge, there is only one study dealing with GHG emissions from fish ponds in temperate latitudes, more precisely with diffuse CH_4 emissions (Rutegwa et al., 2019).

Carp ponds have been excavated in Central and Eastern Europe since the eleventh century, and this aquaculture hardly changed from the Middle Ages until the end of the nineteenth century, when liming, fertilisation and supplementary feeding in the form of pellets and grain increased both fish production and ecosystem degradation (Adámek et al., 2014; Francová et al., 2019; Gál et al., 2016; Geldhauser and Gerstner, 2022; Pechar, 2000). Most of these extensively to semi-intensively managed, natural-looking freshwater fish ponds are several hundred years old, shallow and eutrophic (Potužák et al., 2007). Previous studies focussed on the environmental impact of fish ponds in temperate regions, on eutrophication and biodiversity (Adámek et al., 2014; Pechar, 2000; Rutegwa et al., 2019). Rutegwa et al. (2019) was the first to investigate their climate relevance, but only diffusion as one of the two main GHG transport pathways. To our knowledge, we are the first to investigate diffusive and ebullitive CH_4, CO_2 and N_2O emissions from this type of aquaculture, which is widespread in Europe. We expected high GHG emissions due to the explained physical and biogeochemical properties. We hypothesised that the static feeding sites represent significant GHG hotspots due to the input of fish feed as labile, easily biodegradable OM. To verify this, we compared the GHG emissions from the feeding and a central site in 12 German fish ponds. To identify possible short-term diurnal dynamics, we measured GHG ebullition over two days in the most productive fish pond in a second step. By sampling several sites within this pond, we addressed the spatial variability. In addition, we searched for drivers of the observed CH_4 emissions using a variety of environmental parameters. We therefore address a relevant knowledge gap regarding the GHG impact of aquaculture and also hope to provide incentives for more climate-friendly aquaculture.

2. Methods

2.1 Study site description

The investigated excavated, earthen freshwater fish ponds located near Bautzen, Germany, included 11 extensively to semi-intensively managed fish ponds with low to medium fish stocking and one recently reconstructed carp nursery pond (Table 1, Figure 1). According to the operators, the youngest fish ponds, Teich 1 to 4, were built for fish production between 1950 and 1990; the others are up to 400 yr old and were reconstructed in the 1960s and 1980s. The fish growing season lasted from spring to autumn. In spring, the ponds were filled with water and stocked with fish, which were harvested by drainage in autumn. As sediment accumulates in deeper areas, the internal drainage troughs and harvesting pits with the water discharge were dredged every 3 to 5 yr. However, with the exception of the newly reconstructed carp nursery, no pond was dredged during the last 3 years prior to our study. Fertilisation, liming or aeration did not take place. The fish ponds contained common carp (*Cyprinus carpio*), which were fed grain at stationary feeding sites weekly or twice weekly, as required. Only two fish ponds, the Gerstenteich and the Kleiner (Kl.) Krähenteich, contained catfish (*Silurus glanis*) and tench (*Tinca tinca*), which were fed with fish and plant meal pellets via automatic feeders. These floating feeders carried two pellet containers and dispensed a certain amount of feed into the water below when touched by fish. They rotated around a fixed point covering an area of ~50 m^2. All feeding sites were located at the easily accessible harvest pits, the deepest point of the fish ponds (mean depth: 1.5 ± 0.4 m). Mean water depth at the central sites was 1.0 ± 0.4 m. The ponds were classified as eutrophic (Klaper and Kořínek, 1992), with no significant inflow or outflow of surface water. Some of the fish ponds had high populations of *Elodea* and *Potamogeton* species, partly also green filamentous algae (*Zygnemataceae*), duckweed (*Lemnoideae*) or water lilies (*Nymphaea*). Often the water was greenish due to high algae density (indicated by the shallow Secchi depth). Deciduous trees and reeds surrounded the fish ponds as a narrow belt of littoral vegetation between adjacent grassland and farmland.

Table 1: Characteristics of the investigated 12 freshwater fish ponds: Fish stockings of Common carp or Catfish/Tench (C or S/T plus fish age at the start of the season) at the start and the end of the season. Feed included wheat (or wheat meal in case of the nursery pond; no mark), triticale and fish pellets made from fish/vegetable meal mix**. Organic carbon (OC) content of annual feed quantity, water depth at the feeding (F) and the central sites (M), Secchi depth (measured in June and, in brackets, Sept 2021) and surface area. Data on fish stocking and feed provided by the fishing companies: (a) Forellen- und Lachszucht Ermisch, 01844 Neustadt, (b) KREBA-FISCH GmbH, 02906 Sproitz / Quitzdorf am See, (c) Teichwirtschaft Kauppa, 02694 Kauppa / Großdubrau (part of the Biosphere reserve Oberlausitz).*

Fish pond (abbr.)	**Area**	**Fish stocking** kind/age	start	end	**Feed**	**OC of feed**	**Depth** F	M	**Secchi depth**
	(ha)		(kg/ha)	(kg/ha)	(kg/ha yr)	(g/kg)	(m)	(m)	(m)
Teich 1[a]	15.7	C1	13	136	6,000	415	1.4	1.3	1.3
Teich 2[a]	14.2	C3	134	486	6,700	415	2.5	1.6	0.75
Teich 3[a]	13.3	C3	167	248	8,400	415	1.5	1.5	0.65
Teich 4[a]	10.8	C3	361	583	12,000	415	1.6	1.0	0.85
Brauereiteich[a]	2.2	C3	750	755	2,500	415	1.5	1.1	0.7
Straßenteich[b]	7	C4	430	786	10,010*	407	2.0	1.2	0.35
Gerstenteich[c]	2.5	S2/T2	580	1,600	4,000**	250	1.4	1	0.65 (0.55)

Kl. Krähenteich[c]	3.1	S2/T2	580	1,446	4,000**	250	1.2	0.3	0.45
Al. Krähenteich[c]	5.3	C3	300	471	5,000	415	0.9	0.6	0.2
Inselteich[c]	15	C2	100	433	12,000	415	1.5	0.7	0.65
Thronteich[c]	5.1	C2	50	252	3,000	415	1.3	0.6	1.2
Heikteich[c]	10	Carp nursery	40,000 pc/ha	250	5,000	415	1.3	0.7	0.65

2.2 Field work

We conducted two field campaigns: from 22 to 25 June and from 6 to 10 September 2021. During the survey in June, ebullitive fluxes were measured using bubble traps, inverted funnels with an area of 0.14 m^2 (Figure S.1), at the water surface at two sites per fish pond: One close to the feeding site (for simplicity, hereinafter called “feeding site” (F)), the other 55 m apart in the direction of the centre of the pond (“central site” (M)) (Figure 1). Due to an island in the nursery Heikteich, the distance was here only 35 m. After 24 hours, the gas collected by the funnels was transferred into evacuated exetainer vials (Labco Limited, United Kingdom). If the collected gas volume was too low for later gas chromatography, another 24 hours were added to cover another complete daily cycle. To calculate diffusive fluxes, samples for dissolved concentrations of CH_4, CO_2 and N_2O were taken at the water surface (headspace method). Vertical profiles of water temperature, electrical conductivity, pH, dissolved oxygen (DO), turbidity, and fluorescence-based chlorophyll were acquired by a multiparameter probe (depth interval: 5.0 ± 3.6 cm, Sea & Sun Technologies, Germany). Water transparency was measured using a Secchi disk and samples for water chemical parameters were taken at the central site (s. section 2.4). In addition, samples from the upper 5 cm of the sediment were taken using a gravity corer and PVC liners (UWITEC, Austria, PVC liners of 60 × 9 cm).

In September, we investigated the fish pond with the highest ebullition rate, the Gerstenteich, in more detail. The spatial heterogeneity and diurnal variability of ebullitive CH_4 and CO_2 fluxes were the focus of this second field campaign. Starting from the post of the automatic pellet feeder (site S00), we used a transect of bubble traps into the fish pond (Figure 2). The sites were about 8.5 m apart with 30 m to the last site (S07). The transect covered ~80 m in total. Four additional sites were placed left and right from the transect (S08, S09) and near to the shore left and right (S10, S11). Over two days, the sites were sampled every 3 h between 5:30 a.m. and midnight using evacuated exetainers (Labco Limited, United Kingdom; average duration of complete sampling cycle: 110 min). In addition, due to time constraints, two bubble traps were used for 24-hour measurements, at the feeding site and next to the transect 50 m apart (S01A and S02A). The sampling was accompanied by multiparameter probe profiles at three sites of the transect (S00, S05, S07) and the shore sites (Sea & Sun Technologies, Germany). CH_4 and CO_2 diffusion was measured using a floating chamber connected a portable FTIR analyser (DX4015, Gasmet Technologies, Finland). In addition, water samples for headspace analysis were collected at site S05, around 40 m from S00, as in June. Close by, also the DO concentration was logged in around 35 cm depth and at the ground (RINKO I DO sensors, JFE Advantech Co., Ltd., Hyogo). Weather data was monitored at the pellet feeder by a small weather meter mounted on a tripod (Kestrel 4500, Boothwyn, U.S.A.). At all sites, 5 cm sediment samples were taken.

2.3 Gas analysis and calculations

The analysis of the total gas composition was achieved stepwise by gas chromatography (two different columns) and O_2 measurements directly in the sample vials using a needle-type optode (Firesting, Pyroscience, Aachen, Germany). For CH_4, nitrogen (N_2) and argon (Ar), a gas chromatograph equipped with an aluminium oxide catalyst (5% palladium), a molecular sieve 13X column at 50°C, a flame ionization detector and a thermal conductivity detector was used with hydrogen as carrier gas (SRI-8610C, SRI instruments, Torrance, USA). CO_2 and N_2O were analysed with a HaySep D column at 50°C, a flame ionization detector and an electron capture detector (N_2 as carrier gas). The calibration was adjusted to the concentration range of the respective samples and the injected volume was dependent on the sample volume. For quality control, all relevant bubble gas components were analyzed and summed up (mean 99 ± 2%, single measurements that deviated more than 5% were repeated, data not shown). Since the gas samples were in contact with water, it can be assumed that the missing portion is water vapor (e.g. Boehrer et al., 2021; Horn et al., 2017).

Ebullition rates were calculated by multiplying gas ebullition rates with respective gas concentration in the samples, assuming a molar volume of 24.21 L/mol.

Dissolved CH_4, CO_2 and N_2O concentrations were calculated via eq. 1 from the gas concentrations in equilibrated headspace samples using Henry's Law and temperature corrected solubility coefficients:

$$c_w = c_m \times c_f \times \left(\frac{V_g + \beta \times V_w}{V_w}\right) \qquad \text{with} \qquad c_f = \frac{100}{8.314 \times (T + 273.15)} \qquad \textit{(eq. 1)}$$

c_w is here the concentration of the gas in the water (µmol/L), while c_m is the measured mole fraction of the gas (ppmv). c_f is a conversion factor from mole fraction (ppm) to concentration ($mmol/m^3$) at in situ temperature (T in °C). V_g and V_w are the volumes of the headspace air and water sample used for equilibration and β is the Bunsen solubility calculated using temperature corrected solubility coefficients. Without affecting the water temperature, 30 mL of air and 30 mL of surface water were shaken in a 60 mL syringe for at least one minute. We used an alkalinity based correction for CO_2 and the chemical equilibration of the carbonate system in the vials (Koschorreck et al., 2021).

$$f = k \times (c_w \times c_{eq}) \qquad \text{with} \qquad k = k_{600} \, \frac{\mathrm{Sc}}{600}^{-2/3} \qquad \textit{(eq. 2)}$$

Diffusion fluxes were calculated from the dissolved concentrations c_w using Fick's law (eq. 2). c_{eq} is the equilibrium concentration measured using atmospheric pressure (1.013 bar or measured values) and water temperature, k is the transfer velocity and *Sc* the Schmidt number, defined as the kinematic viscosity of water divided by the diffusion coefficient of a chemical substance contained therein. *Sc* was calculated for the individual gases according to Wanninkhof (1992) as a function of absolute water temperature. k_{600} is the transfer velocity adjusted to a Schmidt number of 600. As the ponds are small, shallow and surrounded by trees, the gas transfer velocity parametrization of Cole et al. (2010) for small lakes under low-wind conditions was used to estimate k_{600}. k for CH_4, CO_2 and N_2O was calculated from k_{600} according to Crusius and Wanninkhof (2003). Total fluxes were calculated as the sum of diffusive and ebullitive fluxes.

Diffusive fluxes measured via floating chambers should be calculated by using linear concentration increases. However, the high background concentration and frequent ebullition events made a quantitative evaluation of the data difficult. For CH_4, only in around 5% of the measurements a continuous linear increase over several minutes could be detected (data not shown). This is why, we use only the headspace derived diffusive fluxes in the following.

To compare the impact of the different GHG and fluxes, we also calculated the global warming potential (GWP) based on the factors given in Neubauer and Megonigal (2015) for CH_4, CO_2 and N_2O diffusion and ebullition of the Gerstenteich in September 2021. That is, we assumed that the effect of CH_4 and N_2O is ~45 and 270 times that of CO_2 over a time horizon of 100 years.

2.4 Water, sediment and pore water analysis

Surface water samples were taken in around 10 cm depth at the central site of the 12 fish ponds during the survey in June 2021. Samples for total bound nitrogen (TN_b), nitrite, nitrate, ammonium (NH_4), total and dissolved organic carbon (TOC and DOC), sulphate and chlorine were filled into a 500 mL brown glass bottles (filtered through pre-muffled 0.7 µm glass fibre filter). Samples for total and dissolved inorganic carbon were filled gas bubble-free into 100 mL brown glass bottles. Samples for magnesium, calcium, sodium, potassium, aluminium, dissolved iron, zinc and manganese were filled into PE-bottles (filtered through 0.45 µm syringe membrane filters). Samples for soluble reactive phosphorus were filled into 250 mL brown glass bottles (filtered through 0.2 µm membrane filters). Total phosphorus (TP) samples were stabilized by adding 1 mL of diluted H_2SO_4 (1:4). All samples were kept refrigerated until analysis. Carbon fractions were analysed IR-spectrometrically using a C-analyser (Dimatec, Germany, Herzsprung et al., 1998). Nitrogen fractions (Herzsprung et al., 2005; Krom, 1980) and soluble reactive phosphorus (Mecozzi, 1995) were measured by continuous flow analysis (CFA, Skalar, Netherlands, Herzsprung et al., 2006). TP was measured photometrically (Skalar, Netherlands). Sulphate and chlorine anions were analysed by suppressed conductivity using an ICS-3000 ion chromatography system (Dionex, Germany) and automatically generated potassium hydroxide eluent. Cations were determined by optical emission spectroscopy with inductively coupled plasma (ICP-OES, Perkin-Elmer, OPTIMA 3000, Germany, Baborowski et al., 2011). Alkalinity were measured by an automatic titrator (Metrohm).

At all sites, sediment samples of the upper 5 cm were taken. Sediment organic matter content and porosity were determined by drying at 60°C and the Loss-on-Ignition method (muffle furnace: 4 h, 500°C). After freeze-drying and homogenisation, total carbon (PC), total organic carbon (POC, after removal of inorganic carbon by acidification), and total nitrogen (PN) were determined by a CN analyser vario EL cube (Elementar Analysensysteme GmbH, Germany). In addition, at the Gerstenteich in September 2021, the sediment was centrifuged to analyse for pore water sulphate by ion-chromatography (Dionex). Pore water DOC and TN_b were analysed using a DIMATOC 2100 (Dimatec, Germany). Since nitrate was below the detection limit in the surface water, we expected that the concentration of this electron acceptor would be below the detection limit in the anoxic pore water (no analyses). In addition, sediment sludge was analysed photometrically (Cary 60 UV-Vis Spectrophotometer, United States) for iron using Ferrozin and Hydroxylammoniumchlorid (Lovley and Phillips, 1987).

2.5 Net ecosystem production

Based on continuous DO concentrations measured in Gerstenteich in September 2021, metabolism calculations were done using the R package LakeMetabolizer (Winslow et al., 2016). Using the Maximum Likelihood method and a mean water depth of 1.2 m, the C input via net ecosystem production (NEP) was estimated. To compare the annual OC input via fish feed and NEP, extrapolations were done for 8 (fish growing phase, afterwards drained) and 12 months.

2.6 Statistics

Software R version 3.5.1 was used for statistical analysis and data visualizations (R Core Team, 2019). To search for significant differences and correlations, paired *t* tests, principal component analyses, non-metric multidimensional scaling and correlation matrices (Spearman's rank) were used on the several data sets (initial fish pond/site-specific variables: Table S.6). We used different types of models (linear models, generalized linear models, linear mixed-effects modelling with e.g. the fish companies as random factor) to investigate possible drivers of CH_4 emissions. However, using the Akaike Information Criterion, linear correlation proved to be the best model type.

3. Results

3.1 Survey - Characterisation and comparison of 12 temperate fish ponds

3.1.1 Chemical and physical parameters of surface water and sediment

Temperature (23.9 ± 1.0°C), pH (7.7 ± 0.4) and water cations and anions contents were in a similar range in the eutrophic to polytrophic fish ponds (Table S.1 and S.2) (Klaper and Kořínek, 1992). Nitrate and nitrite in surface water exceeded the limit of quantification only in Straßenteich. NH_4 concentrations were variable and distinctly higher in Gerstenteich (0.7 mg/L). Soluble reactive phosphor contents were also higher in Gerstenteich and Teich 1. The DO profiles were measured during sampling and thus at different times for the respective ponds (between 7:30 and 20:30). The DO contents averaged over the profiles and those measured near the sediment were 62.5 ± 26.2% and 53.6 ± 26.3%, respectively and were slightly (but not significant, paired *t* test) higher at the feeding sites. Chlorophyll *a* and turbidity varied partly strongly between the sites and the fish ponds but showed no significant differences. The highest mean chlorophyll *a* content of the measured vertical profiles was 130 g/L at the central site of the Gerstenteich. DOC was between 7.0 and 10.9 mg/L (9.5 ± 1.2 mg/L). POC was significantly higher in the feeding site sediments compared to the central sites (63.2 ± 39.5 g/kg dry weight (DW) compared to 26.3 ± 11.6 g/kg DW, recently reconstructed Heikteich excluded) and accounted for 98 ± 3% of the total sediment carbon. This tendency was also true for porosity and PN, which was particularly high at the feeding site of Gerstenteich (16.5 g/kg DW). The C/N ratio was 8.5 ± 2.2.

Table 2: Total, ebullitive and diffusive CH_4, CO_2 and N_2O emissions at the feeding (SF) and central sites (SM) of the survey and at the Gerstenteich in June 2021 (feeding (GF) and central site (GM)) and in Sept. 2021 at site S00, directly at the automatic pellet feeder (GH), the area with (GFA, calculation based on concentric scheme of Fig. 2) and without (GBA) the influence of the feeding site and the Gerstenteich as a whole (G). Given is the mean ± standard deviation, if possible, and the

*share of ebullition (% eb.). *The diffusive fluxes measured at S05 were used as a reference for the diffusion of the whole Gerstenteich.*

		Site / area	SF	SM	GF	GM	GH	GFA	GBA	G
CH_4	Eb.	($mmol/m^2d$)	139 ± 134	9 ± 12	462	42	1238	108	8 ± 7	13
	Diff.	($mmol/m^2d$)	13 ± 7	10 ± 8	19	24	-	-	23 ± 17*	23 ± 17*
	Total	($mmol/m^2d$)	153 ± 138	19 ± 19	481	66	1261	131	31 ± 24	36
	% eb.	(%)	91	48	96	63	98	82	25	35
CO_2	Eb.	($mmol/m^2d$)	6 ± 8	0.3 ± 0.6	30	1.8	177	24	0.1 ± 0.3	0.5
	Diff.	($mmol/m^2d$)	111 ± 68	58 ± 63	184	157	-	-	65 ± 50*	65 ± 50*
	Total	($mmol/m^2d$)	118 ± 72	59 ± 64	214	159	242	90	66 ± 50	66
	% eb.	(%)	5.4	0.5	14	1.2	73	27	0.2	0.8
N_2O	Total	($\mu mol/m^2d$)	6 ± 10	4 ± 10	6.8	4.6	-	-	0.8 ± 0.9*	0.8 ± 0.9*
	% eb.	(%)	3.7 ± 4.6	0.2 ± 0.3	6.3	0.5	-	-	-	-

3.1.2 GHG emissions during the survey - Comparison of feeding and central sites

The investigated 12 fish ponds showed a high variability with significantly higher GHG emissions at the feeding sites (Table 2, bubble gas composition and emission pathways in detail in Table S.3, Figures S.2 and S.3): In addition to one order of magnitude higher ebullition rates, the bubble CH_4 contents at the feeding sites were 77.1 ± 3.6% compared to 51.8 ± 20.5% at the central sites. Mean CH_4 ebullition was 139 ± 134 $mmol/m^2d$, more than 15 times higher than at the central sites (Figure 1). It ranged from 462 mmol CH_4/m^2d at the Gerstenteich feeding site to 0.2 mmol CH_4/m^2d at the central sites of Teich 2 and 4. The variability between the fish ponds was in the same order of magnitude as the CH_4 ebullition itself. The recently reconstructed nursery pond (Heikteich) had lower CH_4 ebullition rates and will be discussed separately.

CH_4 diffusion did not differ significantly between sites, averaging 11.5 ± 7.6 $mmol/m^2d$. Total CH_4 emissions were highest at the Gerstenteich, up to 481 $mmol/m^2d$, while only 3 $mmol/m^2d$ were emitted at the central site of the Alter (Al.) Krähenteich. Ebullition accounted for 84.4 ± 18.2% of the CH_4 emissions at the feeding sites reaching 96% at the Gerstenteich feeding site. But at the central sites, ebullition was only half as important (38 ± 25%) and the dominance of the pathways changed.

CO_2 emissions varied greatly between fish ponds and sites: from undersaturated conditions (theoretical CO_2 uptake, autotrophic) to emission of 213.6 $mmol/m^2d$ at the Gerstenteich feeding site. Diffusion was clearly the dominant pathway (96.9 ± 3.9% of heterotrophic CO_2 emissions). CO_2 ebullition and diffusion were significant higher at the feeding sites where mean CO_2 emission was twice as high with 118 ± 70 mmol/m^{2}d. CO_2 ebullition was highest at the Gerstenteich feeding site.

Bubble N_2O contents ranged between 0.2 and 1.8 ppm and ebullitive fluxes were negligible. Diffusion was with 97.9 ± 3.8% the main pathway but N_2O uptake was also observed. N_2O emissions ranged from -7.0 µmol/m^{2}d (central sites of Teich 3 and 4) to 32.1 µmol/m^{2}d (Straßenteich). However, without these values, mean N_2O emission was 3.3 ± 3.9 µmol/m^{2}d with no significant difference between sites.

Emissions at the recently reconstructed carp nursery pond had a different pattern. At the central site of the Heikteich, the ebullition rate was higher than at the feeding site. However, as the CH_4 content of the bubbles was very low at 1.6%, CH_4 ebullition was still higher at the feeding site. The CH_4 ebullition rate at the feeding site was comparable to that at the central sites of the other fish ponds - as were CH_4 and CO_2 diffusion and total emission. N_2O emissions were similar to the other fish ponds.

3.2 Detailed study at the Gerstenteich

3.2.1 Chemical and physical parameters of water, sediment and pore water

While the pH was in the same range as in June, the water temperature was 6°C lower at 19.2 ± 0.7°C (Table S.4). Trends with distance from the feeding site S00 were more pronounced for pore water DOC and TN_b than for POC, PN or their C/N ratio (mean C/N: 7.3 ± 1.3). Figures S.4, S.5 and S.6 show CTD-profiles and contour plots of water temperature, DO and chlorophyll at S00, S05 and S07, the beginning, middle and end of the transect into the Gerstenteich. On both days, stratification built up during the day and disappeared at night. The DO content was lowest at the feeding site reaching values down to 30% in the early morning hours near the sediment and increased with distance from the feeding site. Although there was no clear trend in turbidity and chlorophyll concentration, higher DO maximum values were reached at S05 and S07 in the early afternoon. Near S05, the diurnal DO ranged from 33% to 161% at 35 cm depth, but remained close to 0% at the sediment surface (Figure

S.7). Diurnal temperature variations at both depths were small. Wind speed was mostly below 1 m/s and slightly higher on the second day when also air pressure dropped by 6 mbar (Figure S.8).

Based on the DO measurements, the NEP was determined to be 0.1 mg C/Ld. Extrapolated to 8 months of fish production, NEP accounted for only 17% of the annual OC input via fish feed. Since our measurements took place in September and higher DO values could be expected in summer, we also made an estimate for 12 months, as a maximum estimate. The share was 26%.

3.2.2 Spatial heterogeneity of ebullition

By using a transect of bubble traps and additional sites in the Gerstenteich, we were able to identify a clear ebullition pattern influenced by the feeding site. Directly at the automatic pellet feeder (S00), an ebullition rate of 38 L/m^{2}d with a mean bubble CH_4 content of 79 ± 11 % was observed (Figure S.2 and Table S.5). The resulting CH_4 ebullition was 1.24 mol/m^{2}d (Table 2). CH_4 ebullition declined exponentially with distance to the feeding site due to both, reduced ebullition rates and bubble CH_4 contents (Figure 2). This resulted in a feeding site influenced area of about 40 m diameter. Outside this area, which is referred to as background in the following, CH_4 ebullition was less than 1% of the rate at site S00. This means that the variability within the ecosystems was of the same order of magnitude as the ebullitive CH_4 flux itself and that 40% of the total CH_4 ebullition occurred in < 5% of the area. Mean CH_4 diffusion measured at S05 was 23 ± 17 mmol/m^{2}d and was thus comparable to the diffusive flux determined in June. Based on this value, we estimated a CH_4 emissions rate of 36 mmol/m^{2}d for the whole Gerstenteich. While ebullition accounted for 82% of the total CH_4 emissions from the area influenced by the feeding site, its importance for the entire fish pond was significantly lower at 35%.

At S00, the bubble gas also contained CO_2 in significant proportions leading to a CO_2 ebullition of almost 400 mmol/m^{2}d at high times and a mean value of 177 mmol/m^{2}d. However, CO_2 ebullition decreased faster than CH_4 ebullition with increasing distance from the feeding site, resulting in a feeding site influenced area of about 12 m radius and a negligible background CO_2 ebullition flux, which was lower by a factor 500. This means that in < 2% of the area 79% of the total CO_2 ebullition occurred. Mean CO_2 diffusion at S05 was with 66 ± 50 mmol/m^{2}d lower than in June, but accounted for 99% of the CO_2 emissions. N_2O diffusion at S05 was low with 0.8 ± 0.9 µmol/m^{2}d.

3.2.3 Diurnal variability of ebullition

We observed considerable temporal variability of CH_4 ebullition (Figure 3). The picture seemed heterogeneous, but at the second sampling, between 5:30 and 10:30 in the mornings, 90% of the sites had CH_4 ebullition rates above the site mean CH_4 ebullition value. This pattern occurred on both days. If the CH_4 ebullition was calculated separately for both days according to the concentric scheme in Figure 2, there was only a slight deviation of 3.3% or 11 mol CH_4. Figure 4 shows diffusive and ebullitive CH_4 and CO_2 fluxes at site S05, 42 m from S00. Total CH_4 and CO_2 emissions were highest at night and in the morning. N_2O diffusion was low and showed no distinct diurnal pattern (data not shown). Although the floating chamber measurements were difficult to evaluate due to the high ebullition rates, the trends and ranges observed for CO_2 diffusion confirmed our headspace measurements (data not shown).

3.3 Global warming potential

The GWP of the Gerstenteich for both days in September 2021 was 28.7 g CO_2-eq/m^{2}d or 0.65 mol CO_2-eq/m^{2}d. While N_2O fluxes and CO_2 ebullition were negligible (accounting for 0.03% and 0.1%), CO_2 diffusion accounted for 10.1% of the GWP. CH_4 accounted for almost 89.9%, 58.4% emitted by diffusion and 31.5% by ebullition.

3.4 Drivers of CH_4 emissions

In contrast to CH_4 diffusion and N_2O fluxes, CH_4 and CO_2 ebullition, bubble gas composition (mainly CH_4 and N_2), CO_2 diffusion, and total CH_4 and CO_2 emission differed significantly between the feeding and central sites. The factor "feeding site" or "central site" explained 55% of the variance in the CH_4 ebullition flux. Other factors like "high/low abundance of macrophytes" or "fishing companies" (possible management differences) were not significant. Significant differences between the survey feeding and central sites were found only for the sediment parameters POC and PN and for water depth. Linear correlation analyses showed that sediment associated parameters were important drivers for the CH_4 emissions (Table 3 and S.6 with an overview of the parameter variety of the modelling). PN and POC clearly correlated with CH_4 ebullition when survey feeding and central sites were taken into account (PN: R^2 of 0.62, $p < 0.001$; POC: R^2 of 0.32, $p < 0.005$). This pattern was also true when the feeding sites were modelled separately (PN: R^2 of 0.55, $p < 0.005$). However, at the central sites, PN or POC correlated only weakly with CH_4 ebullition while chlorophyll *a* was the strongest predictor (R^2 of 0.44, $p < 0.05$) followed by the amount of fish at the end of the season (R^2 of 0.39, $p < 0.05$). Especially at the central sites, chlorophyll *a* correlated strongly with the amount of fish at the beginning and the end of the season (R^2 of 0.62 and 0.79, both $p < 0.001$), as well as with the annual input of OC via fish feed (R^2 of 0.38, $p < 0.05$). The amount of fish at the beginning of the season or the annual input of OC or N via the fish feed did not correlate significantly with CH_4 ebullition. But we identified NH_4 in surface water as a strong proxy of CH_4 ebullition, both at the feeding and central sites (both: R^2 of 0.77, $p < 0.001$). While DO correlated with CH_4 ebullition at the feeding sites (R^2 of 0.41, $p < 0.05$), there was no significant correlation at the central sites.

The sites of the detailed Gerstenteich study covered both, areas with and without the influence of the feeding site. Pore water TN_b and DOC had adjusted R^2 values of 0.98 and 0.92 when correlated with CH_4 ebullition ($p < 0.001$). Just like PN and POC, TN_b and DOC were strongly intercorrelated. Solid-phase PN and POC were not significantly correlated with the observed CH_4 ebullition and even when CH_4 ebullition data from both field campaigns were combined, the R^2 of PN was only 0.14 ($p < 0.05$). Furthermore, there was no correlation between the C/N ratio and CH_4 emissions. Water temperature near the sediment was very similar between the sites and thus did not explain spatial variability of ebullition. Although also the water depth was quite similar at the different sites, there was a positive correlation with the emissions.

Table 3: Linear modelling of CH_4 ebullition, diffusion and total emission via environmental variables for the survey feeding (SF) and central sites (SM) as well as the Gerstenteich (G). Number of included sites (n) and adjusted R^2 with a significance of

$p < 0.001$. Drivers are sediment organic carbon (POC) and nitrogen (PN), ammonium (NH_4), dissolved oxygen (DO), chlorophyll a (Chl.A), pore water dissolved organic carbon (PW.DOC) and total bound nitrogen ($PW.TN_b$).

Parameter	Sites	Linear modelling	n	R^2
CH_4 ebullition	SF & SM	$0.7\ PN + 0.3\ NH_4 - 0.3\ DO$	24	0.72
	SF	$0.4 + 0.6\ NH_4 - 0.5\ DO + 0.3\ PN$	12	0.87
	SM	$-0.5 + 0.08\ NH_4 + 0.03\ Chl.A$	12	0.81
	G	$115.7 + 323.5\ PW.TN_b$	12	0.98
CH_4 diffusion	SF & SM	$0.6\ PW.DOC - 0.5\ NH_4 + 0.3\ POC$	24	0.74
CH_4 emission	SF & SM	$0.7\ PN + 0.2\ NH_4$	24	0.70

4. Discussion

4.1 GHG emissions from temperate freshwater fish ponds

Before we go into the interpretation of the data, it is important to clarify the explanatory power of our investigations: Due to the high spatiotemporal variability of GHG emissions, especially ebullition, flux measurements at one site are not sufficient to describe an ecosystem in a representative way (e.g. Wik et al., 2016). Nevertheless, the mean values of our survey provide a benchmark to compare these 12 temperate, extensively to semi-intensively used fish ponds with other aquaculture and natural ponds and to assess the impact of feeding sites. They reflect trends and orders of magnitude, which are then investigated representatively in our detailed study on the Gersteneich. Here, the focus was placed specifically on the ebullitive gas transport pathway. In addition, we studied the ponds during the fish growing season in June and September 2021, not covering the period of winter drainage when redox conditions in the sediment may change, resulting in lower CH_4 but possibly increased CO_2 and N_2O emissions (Madigan and Martinko, 2006).

*Table 4: GHG emissions from aquaculture systems, urban ponds and other water bodies in comparison to the semi-intensively managed Gersteneich in Sept. 2021. *Diffusive fluxes measured at S05 as a reference for the diffusion of the whole fish pond. Given is the mean ± standard deviation or the range as in the references. FW abbreviated for freshwater, aquac. for aquaculture and maric. for mariculture. Given are current review articles on aquaculture with a focus on freshwater systems, relevant case studies on aquaculture and urban ponds, and reviews on natural ecosystems.*

Ecosystem	CH_4 emissions (mmol/m²d)	CH_4 Diffusion (mmol/m²d)	CH_4 Ebullition (mmol/m²d)	CO_2 emissions (mmol/m²d)	N_2O emissions (µmol/m²d)	Literature
FW fish pond, Germany	36	23 ± 17*	13	65 ± 50*	0.8 ± 0.9*	This study
Feeding site hotspot	1261	23 ± 17*	1238	65 ± 50*	0.8 ± 0.9*	

Aquac., extensive	6.6 ± 10.3	-	-	-	4.1 ± 3.7	Kosten et al. (2020)
Aquac., semi-intensive	15.0 ± 6.6	-	-	-	15.3 ± 17.7	
FW aquac. ponds	27.4 ± 36.8	-	-	-	-	Rosentreter et al. (2021
Aquac., China	-0.01 to 129	-	-	-87 to 126	-	Zhang et al. (2022)
Inland aquac. ponds, China	9.2 ± 3.3	-	-	24.5 ± 5.4	-	
Lake/reservoir aquac., China	1.4 ± 0.8	-	-	24.6 ± 6.6	-	
Rice-field, China	6.7 ± 1.0	-	-	116.2	-	
Aquac., China	10.0 ± 3.0	-	-	-	-	Dong et al. (2023)
FW fish pond, Czech	-	0.53 ± 0.57	-	-	-	Rutegwa et al. (2019)
FW fish ponds, India	37.2 ± 18.0	-	-	-	-	Shaher et al. (2020)
FW fish pond, China	1.4	0.2	1.2	-	11.4	Fang et al. (2022a, b)
FW carb ponds, China	16.5 ± 1.1	-	-	0.8 to 12.4	-	Yuan et al. (2019)
FW crab ponds, China	13.5 to 21.5	2.7 to 3.5	10.8 to 18.0	-	< 5	Yuan et al. (2021)
Shrimp maric., China	23.9	2.4	21.5	-	-	Yang et al. (2020)
Coastal shrimp ponds, China	33.9 ± 10.4	3.4 ± 1.0	30.5 ± 9.3	10.0 ± 4.0	-	Tong et al. (2021)
Urban ponds, Germany	26.2 ± 36.2	7.5 ± 1.0	18.7 ± 35.2	-	-	Ortega et al. (2019)
Urban pond, Netherlands	10.6	2.1	8.6	80.4	-	van Bergen et al. (2019)
Water retention ponds, USA	5.5 to 53.1	-	-	12 to 115	7.3 to 70.3	Gorsky et al. (2019)
Urban ponds, Sweden	-	1.9	-	17.1	-	Peacock et al. (2019)
Agricultural ponds, Canada	-	0.14 to 92	-	-21 to 466	-12 to -2	Webb et al. (2019a, b)
Common FW ponds, India	17.9 ± 18.5	3.1	14.8	67.1 ± 64.0	-	Selvam et al. (2014)
Natural FW ponds, Canada	-	-	21.7 ± 15.4	-	-	Baron et al. (2022)
Natural lakes <0.001 km²	-	3.1 ± 0.7	-	9.6 ± 1.4	-	Holgerson and Raymond (2
Lakes <0.001 km²	25.4 ± 14.8	-	-	-	-	Rosentreter et al. (2021
Lakes	9.2 ± 2.6	-	-	-	-	

4.1.1 Methane emission

During our field campaigns, we observed a wide range of CH_4 emissions with a remarkable inter- and intra-ecosystem variability - especially with respect to ebullition. The feeding sites were striking CH_4 hotspots with previously unknown ebullitive fluxes of up to 1.81 mol/m^{2}d at the Gerstenteich (site mean value over 48h: 1.24 mol/m^{2}d). And CH_4 diffusion was also high compared to other aquaculture systems, urban ponds or small water bodies (Table 4). In the Gerstenteich, CH_4 diffusion was comparable in June and September 2021 and was additionally verified by floating chamber measurements. With both fluxes, total CH_4 emissions were calculated. CH_4 emissions from aquaculture are influenced by the type of management, the species cultivated and the environmental conditions and therefore span a considerable range, leading to large uncertainties in GHG emission estimates from aquaculture (Dong et al., 2023; Kosten et al., 2020; Rosentreter et al., 2021; Zhang et al., 2022). The reviews currently available mainly refer to aquaculture of crab, shrimp or mixed shrimp-fish systems, with a clear focus on Chinese aquaculture. Mean CH_4 emissions of the central sites of the survey and the result of the detailed Gerstenteich study at the end of the fish growing season in September, where ebullition was recorded not only with the variability inherent of the system, but also with the intensity and spatial extent of the feeding site, were in the upper range of values reported for aquaculture. The 36 mmol/m^{2}d of the entire Gerstenteich in September were higher than the CH_4 emission currently reported by Rosentreter et al. (2021) for lakes with an area of less than 0.001 km^2 and were more than double the top end value for natural freshwater ecosystems of Bastviken et al. (2011). This shows that the natural-looking, temperate fish pond emitted more CH_4 than natural systems, despite its semi-intensive use and even if the hotspot of the feeding site is excluded. A comparison of the ebullition rates of the pond centre in June and September also suggests that CH_4 emissions have already decreased due to the 6°C lower temperature of the water column.

Most aquaculture studies examining both gas pathways report that ebullition was the predominant pathway, accounting for 70-99% of the total CH_4 flux (Tong et al., 2021; Yang et al., 2020; Yuan et al., 2021; Zhao et al., 2021). We observed a wide range regarding the relative importance of ebullition but comparable high shares were only linked to the high total CH_4 emission at the feeding sites. Nevertheless, ebullition proved to be a significant transport mechanism for CH_4, accounting for 35% of emissions from the Gerstenteich in September (> 310 mol daily).

4.1.2 Carbon dioxide emission

For aquaculture systems a wide range of CO_2 emissions is reported, equally so for urban and agricultural ponds, and our results fall with -12 to 242 mmol/m^{2}d within this range (Table 4). CO_2 emissions in this range were also reported for lakes, reservoirs, rivers or beaver ponds (Deemer et al., 2016; Lazar et al., 2014; Rõõm et al., 2014; Selvam et al., 2014; Teodoru et al., 2012; Zhang et al., 2020). During the survey, CO_2 emissions at the feeding sites were twice as high as at the central sites. As expected, due to its high water solubility, diffusion was the main pathway for CO_2 (Boehrer et al., 2021), but at the feeding sites also ebullition played a role. So far, CO_2 ebullition has not been considered in GHG studies but, in the case of the Gerstenteich, CO_2 ebullition directly at the automatic pellet feeder was with 177 mmol/m^{2}d surprisingly high and accounted for 73% of the total CO_2 flux. It is plausible that the CO_2 was produced anaerobically, since similar amounts of CH_4 and CO_2 are produced during the mineralisation of OM under methanogenic conditions (Schwoerbel and Brendelberger, 2016). Obviously, methanogenesis rates were sufficiently high to override the high water solubility and significantly increase the partial pressure of CO_2 in the sediment pore water. Nevertheless, the CH_4 emissions at the Gerstenteich feeding site were more than 5 times higher than the CO_2 emissions. This can be attributed to the high solubility, the carbonate buffer system and the uptake of CO_2 into the biomass of phototrophic organisms (Schwoerbel and Brendelberger, 2016). Assuming that CH_4 emission of 36 mmol/m^{2}d reflected the average methanogenesis rate (steady state), that CH_4 and CO_2 were produced anaerobically in equal parts and that there were no additional CO_2 sources, our NEP calculation allows to estimate the proportion of methanogenically formed CO_2 that is incorporated into the biomass at 69%. It is therefore an important sink in these eutrophic waters. It can be assumed that the emitted CO_2 originated from the easily biodegradable fish feed, feces, and aquatic primary production (Kosten et al., 2020).

4.1.3 Nitrous oxide

Since an increase in N_2O emissions with N load have been observed in lotic systems (e.g. Seitzinger et al., 2000), high N_2O emissions were originally also expected from aquacultures (Hu et al., 2012). N_2O is formed as a by-product during aerobic nitrification or through incomplete denitrification under conditions that are not completely oxygen free (Schlesinger, 2009). However, the low redox potentials in anaerobic sediments favour complete denitrification and result in NH_4 accumulation and NO_3 depletion, which also limits denitrification rates. Therefore, N_2O in lakes and ponds is mainly produced in the epilimnion or at the epilimnion-hypolimnion interface as a by-product of nitrification and, compared to oxygenated and well mixed lotic ecosystems, N_2O emissions are often low (Beaulieu et al., 2015; Deemer et al., 2011; Kosten et al., 2020; Malyan et al., 2022; Webb et al., 2019; Yuan et al., 2021). For example, Baulch et al. (2011) observed N_2O emissions of 776 ± 61 mmol/m^{2}d in streams in Canada, while N_2O uptake was observed in the majority of 101 highly eutrophic, agricultural ponds (Webb et al., 2019) and was reported for more than 40% of the boreal aquatic ecosystems studied in Soued et al. (2016). In addition, N_2O can be consumed in aquatic systems by e.g. denitrifiers and a downward N_2O diffusion gradient into the hypolimnion was assumed (Beaulieu et al., 2015; Deemer et al., 2011; Soued et al., 2016; Webb et al., 2019; Yuan et al., 2021). In line with these findings and other aquaculture studies (Table 4), the investigated fish ponds were only weak N_2O sources with very low emissions during the fish growing season ranging from small N_2O uptake to 32 µmol/m^{2}d in one fish pond. It is therefore becoming increasingly clear that despite intensive N loads and cycling in aquacultures and fish ponds, N_2O emissions are of rather minor importance.

4.1.4 Global warming potential of the Gerstenteich

In order to compare the impact of the different GHG and fluxes, we calculated the GWP to 28.7 g CO_2-eq/m^{2}d. While CO_2 ebullition was negligible, CO_2 diffusion accounted for around 10% of the GWP. The contribution of N_2O as the most potent GHG was negligible (Myhre et al., 2013). CH_4 was clearly the most important GHG, with ebullition responsible for more than a one-third of the GWP fraction of CH_4. This strong dominance of CH_4 is consistent with studies on artificial stormwater ponds, where CH_4 accounted for 94% of the GWP, CO_2 was the second most important greenhouse gas and N_2O was <1% (Gorsky et al., 2019). Yuan et al. (2019) also attributed the significant increase in GWP following the conversion of paddy rice fields to extensively managed crab aquaculture ponds mainly to increased CH_4 emissions.

4.2 CH_4 ebullition - Spatiotemporal variability and differences between fish ponds

CH_4 was clearly the predominant GHG in the observed fish ponds, and a large proportion of the emissions were caused by ebullition. In line with other literature on ebullition (e.g. Beaulieu et al., 2016; DelSontro et al., 2016; Wik et al., 2016), significant differences were observed between the fish ponds and a considerable spatiotemporal variability was found within a single pond. This heterogeneity led to great uncertainties in climate impact assessments and is therefore the subject of the following sections.

4.2.1 Spatial heterogeneity of CH_4 ebullition

Our traditional fish ponds had stationary feeding sites where grain or pellets were dispensed. Since these feeding sites were the deepest parts of the fish ponds and this was where the water was drained for harvesting, sludge and fine sediment could accumulate (Avnimelech and Ritvo, 2003; Boyd et al., 2010). Here, we observed 15.5 times higher ebullitive fluxes and 8 times higher total emissions. Similarly, the feeding site influenced area of the Gerstenteich emitted 13.5 times more CH_4 via ebullition than the background. In less than 5% of the area 40% of the CH_4 ebullition and 16% of the total CH_4 emission occurred. Up to 5 times higher emissions at the feeding zones were also reported for Chinese aquaculture (Fang et al., 2022a; Yang et al., 2020; Zhao et al., 2021) but the differences were not in these dimensions. Directly at the automatic pellet feeder of the Gerstenteich, CH_4 ebullition in September was 155 times as high as the background flux and, at times, more than 2 mol CH_4/m^2d was emitted.

With the exception of water depth, only sediment OC and PN contents (both highly intercorrelated) were significantly different between the survey feeding and central sites. Although the ponds were generally rich in OM and had a low C/N ratio, unconsumed feed and fish feces can accumulate around the feeding site due to the low C utilization efficiency of the fish (Avnimelech and Ritvo, 2003; Rutegwa et al., 2019). The N-rich OM contains large amounts of starch and proteins and is easily bioavailable and rapidly degraded to methanogenic substrates (Yuan et al., 2019). Therefore, previous studies have already shown a good correlation between PN and CH_4 production or emission, especially in OM-rich ecosystems (Gebert et al., 2006; Isidorova et al., 2019). PN explained 62% and 55% of the CH_4 ebullition variability for the survey and the survey feeding sites but for the central sites chlorophyll *a* had much higher predictive power, explaining 44%. We assume that, outside the feeding site influenced area, aquatic primary production was the primary source of the quickly consumed, labile OM used for CH_4 production. Autochthonous OM is (in comparison to allochthonous OM) also rich in protein and relatively easily transformed into CH_4 (Grasset et al., 2018; West et al., 2012).

Fish stocking and feed use correlated only weakly with the measured CH_4 emissions and were outperformed by other predictors. The comparison between the neighbouring fish ponds Kl. Krähenteich and Gerstenteich also showed that neither the fish species nor the type of feed allowed direct conclusions to be drawn about CH_4 emissions. Despite the same catfish/tench stocking and feed quantity, the CH_4 ebullition rates were 5 to 11 times higher at the Gerstenteich than at the Kl. Krähenteich. However, the PN values in the sediment of the Gerstenteich were twice as high. While the CH_4 emissions of the Kl. Krähenteich were in the middle range, the carp pond Straßenteich (grain-fed) had the second highest emissions. The low CH_4 emissions at the Heikteich, the freshly homogenised carp nursery pond, also pointed to the importance of the labile OM input.

Negatively correlated DO played a role at the feeding sites of the survey, where DO levels dropped to only about 30% saturation in the early morning hours due to high respiration. Methanogenesis is an anaerobic process. However, redox conditions at the water-sediment interface change at the microscopic level (e.g. Meijer and Avnimelech, 1999; Phan-Van et al., 2008), and variable DO content in the water column therefore does not appear to be a reliable predictor of CH_4 production and emission. Due to the narrow temperature range, temperature did not have the reported strong effect (e.g. Fuchs et al., 2016) but the temperature difference of 6°C between June and September could explain the higher CH_4 ebullition rate at the Gerstenteich central site in June.

At the Gerstenteich, where feeding site influenced (4) and central sites (10) were combined, correlations showed that not the sediment solid phase, but the pore water TN_b and DOC contents explained the measured CH_4 ebullition to astonishing 98% and 92%. Labile pore water OM derived from fish feed and feces as well as from primary production determined the observed CH_4 ebullition. Correlations between chlorophyll *a* and fish abundance or OC input via fish feed indicated a fertilization effect as reported by Flickinger et al. (2020), but, analogous to Yuan et al. (2019), our extrapolations (on the basis of 8 months) showed that annual OC input via fish feed accounted for about 85.4% of the total OC inputs. It is natural to assume that the fish pellets with a C/N ratio of 3.2 (data not shown) contained even more easily degradable proteins and organic acids than the phytoplankton (assuming a C/N ratio of 6.6 based on the Redfield ratio; Redfield, 1958). Since the C/N ratio of the sediment was comparable for all sites (mean at the Gerstenteich: 7.3 ±1.3) and also for the different fish ponds (mean during the survey: 8.5 ± 2.2), these substances were consumed so quickly that, despite the high input, the sediment solid phase was not permanently altered. The high emissions near the feeding site can therefore be explained by the high, punctual input of very easily biodegradable OM. This would mean that methanogenesis in these OM- and nutrient-rich fish ponds was still limited by (the quality of) the substrate, as has been demonstrated for many other ecosystems and sites (e.g. Bastviken, 2009). The positive correlation with water depth, on the other hand, seems to be an artefact of the strong OM influence, since with increasing depth also the absolute pressure increases, which must be overcome to form bubbles (Boehrer et al., 2021). In addition, NH_4 proved to be a strong and easily measured indicator of CH_4 emissions during the survey. NH_4 is a mineralisation product related to reducing redox conditions and a part of the TN_b measured in the pore water of the Gerstenteich (Madigan and Martinko, 2006).

4.2.2 Temporal variability of CH_4 ebullition

In the morning, between 8:30 and 10:30 a.m., we observed higher rates of CH_4 ebullition that could not be explained by physicochemical conditions in the water and atmosphere. DO in the water column, lowest during the first sampling, were already rising slightly during this period, atmospheric pressure and wind were inconspicuous, and temperature variations were small over the entire period (Table S.4, Figures S.5, S.7 and S.8). This points to bioturbation as trigger of CH_4 ebullition. Bioturbation can influence redox conditions and physicochemical parameters in the sediment that regulate the production, transport and consumption of CH_4 (Bezerra et al., 2020; Oliveira Junior et al., 2019). The effects of bioturbation on ebullition and GHG emissions are complex and discussed contradictorily in the literature. On the one hand, bioturbation by benthivorous fish can oxygenate water column and sediment and reduce the production of CH_4 or toxic reduced species such as hydrogen sulphide (Adámek and Maršálek, 2013; Joyni et al., 2011; Oliveira Junior et al., 2019; Rutegwa et al., 2019). OM accumulation is reduced and fish productivity is increased due to the better soil and water conditions (Joyni et al., 2011). Oliveira Junior et al. (2019) observed a decrease in CH_4 emissions of 62.1% in mesocosm experiments with and without benthivorous fish. It is also assumed that the continuous disturbances prevent the bubble build-up. In contrast, a large number of studies described increased ebullition rates for fish and other benthivorous fauna because bubble release would be triggered by physical disturbances (Bezerra et al., 2020; Datta et al., 2009; Frei and Becker, 2005; Leal et al., 2007). And Yuan et al. (2021) reported optimal redox conditions for methanogenesis despite crab bioturbation. As in this study, Bezerra et al. (2020) suggested that diurnal CH_4 emission patterns are shaped by the specific activity patterns of benthivorous fauna. The overall effect of bioturbation on GHG emissions is therefore difficult to predict. So is the maximum activity and distribution areas of certain benthivorous fish species like catfish (e.g. Říha et al., 2021). Some studies (e.g. Long et al. 2016) examined ebullition over shorter time spans than 24 hours, often during the morning. When ebullition rates at the Gerstenteich were measured only between 8:30 a.m. and 1:00 p.m., total CH_4 ebullition would have been overestimated by 55%. Thus, for a correct quantification of ebullition, the bubble traps need to be deployed over a complete 24h cycle.

5 Conclusion

Global climate change is one of the main challenges of our time but current estimates of the climate impacts of aquaculture come with huge uncertainties. This study is the first to quantify both diffusive and ebullitive greenhouse gas emissions from freshwater fish ponds in a temperate climate. At the stationary feeding sites of the investigated extensively to semi-intensively managed fish ponds, CH_4 emissions of up to 2 mol/m^{2}d were observed. CH_4 was the most important greenhouse gas and accounted for ~90% of the global warming potential in one pond. Ebullition, the gas flux via bubbles, clearly dominated the CH_4 emissions at the feeding site hotspots. Here, unconsumed feed and fish feces promoted mineralization and resulted in, to our knowledge, the highest rates of CH_4 and CO_2 ebullition reported to date from natural or aquaculture ecosystems. We therefore conclude that ebullition and the feeding site must be considered for robust quantification, otherwise greenhouse gas emissions from aquaculture are significantly underestimated. For the 2.5 ha Gerstenteich, excluding ebullition would reduce anthropogenic CH_4 emission estimates by 35% and not including the feeding site would result in a 15% error. We observed high spatiotemporal variability among and within the fish ponds with respect to ebullition, which was mainly due to nitrogen-rich and easily degradable organic matter and presumably bioturbation. Despite high organic nitrogen loads, N_2O emissions were insignificant, probably because of the strongly reducing conditions in the sediment. We hope to trigger strategies for a more climate-friendly fish industry and see the potential to adapt traditional fish pond management through more efficient feeding and reduced accumulation of organic matter.

Declaration of Competing Interest

The authors declare that they have no known competing financial interests or personal relationships that could have appeared to influence the work reported in this paper.

Data availability

Data is available in the extensive appendix. If further data is required, it will be provided upon request.

Acknowledgment

We thank Martin Wieprecht, Thomas Bechle, Hannah Mihm, and Patrick Aurich for their eminent help during field and laboratory work. Further we thank Bertram Boehrer, Peifang Leng, and Michael Seewald for their constructive input and advice. In addition, Andrea Hoff on behalf of the GEWANA team is acknowledged for analysing water, sediment, and pore water parameters. This research was financially supported by the German Research Foundation (DFG) (Grant number KO 1911/7-1).

We thank the expert reviewers for their valuable and constructive comments and the fish companies for the support and fruitful cooperation.

Appendix A. Supporting Information

Supplement data associated with this article can be found in the online version at doi…

5. References

Adámek, Z., Helešic, J., Maršálek, B., Rulík, M., 2014. Applied Hydrobiology. Univ.South Bohemia in České Budějovice.

Adámek, Z., Maršálek, B., 2013. Bioturbation of sediments by benthic macroinvertebrates and fish and its implication for pond ecosystems: a review. Aquac. Int. 21, 1–17. https://doi.org/10.1007/s10499-012-9527-3

Avnimelech, Y., Ritvo, G., 2003. Shrimp and fish pond soils: processes and management. Aquaculture 220, 549–567. https://doi.org/10.1016/S0044-8486(02)00641-5

Baborowski, M., Büttner, O., Einax, J.W., 2011. Assessment of Water Quality in the Elbe River at Low Water Conditions Based on Factor Analysis. CLEAN – Soil Air Water 39, 437–443. https://doi.org/10.1002/clen.201000373

Baron, A.A.P., Dyck, L.T., Amjad, H., Bragg, J., Kroft, E., Newson, J., Oleson, K., Casson, N.J., North, R.L., Venkiteswaran, J.J., Whitfield, C.J., 2022. Differences in ebullitive methane release from small, shallow ponds present challenges for scaling. Sci. Total Environ. 802, 149685. https://doi.org/10.1016/j.scitotenv.2021.149685

Bastviken, D., 2009. Methane. Elsevier, pp. 783–805.

Bastviken, D., Cole, J., Pace, M., Tranvik, L., 2004. Methane emissions from lakes: Dependence of lake characteristics, two regional assessments, and a global estimate. Glob. Biogeochem. Cycles 18. https://doi.org/10.1029/2004GB002238

Bastviken, D., Tranvik, L.J., Downing, J.A., Crill, P.M., Enrich-Prast, A., 2011. Freshwater Methane Emissions Offset the Continental Carbon Sink. Science 331, 50–50. https://doi.org/10.1126/science.1196808

Baulch, H.M., Schiff, S.L., Maranger, R., Dillon, P.J., 2011. Nitrogen enrichment and the emission of nitrous oxide from streams: NITROUS OXIDE EMISSIONS FROM STREAMS. Glob. Biogeochem. Cycles 25, n/a-n/a. https://doi.org/10.1029/2011GB004047

Beaulieu, J.J., McManus, M.G., Nietch, C.T., 2016. Estimates of reservoir methane emissions based on a spatially balanced probabilistic-survey. Limnol. Oceanogr. 61, S27–S40. https://doi.org/10.1002/lno.10284

Beaulieu, J.J., Nietch, C.T., Young, J.L., 2015. Controls on nitrous oxide production and consumption in reservoirs of the Ohio River Basin. J. Geophys. Res. 16.

Beaulieu, J.J., Waldo, S., Balz, D.A., Barnett, W., Hall, A., Platz, M.C., White, K.M., 2020. Methane and Carbon Dioxide Emissions From Reservoirs: Controls and Upscaling. J. Geophys. Res. Biogeosciences 125, e2019JG005474. https://doi.org/10.1029/2019JG005474

Bezerra, M.P., McGinnis, D.F., Bezerra-Neto, J.F., Barbosa, F.A.R., 2020. Is it stochastic? Chaoborus larvae bioturbation likely affect the timing of daily methane (CH4) ebullitive flux in a tropical reservoir. Hydrobiologia 847, 3291–3308. https://doi.org/10.1007/s10750-020-04331-w

Boehrer, B., Jordan, S., Leng, P., Waldemer, C., Schwenk, C., Hupfer, M., Schultze, M., 2021. Water | Free Full-Text | Gas Pressure Dynamics in Small and Mid-Size Lakes [WWW Document]. URL https://www.mdpi.com/2073-4441/13/13/1824 (accessed 3.24.22).

Boyd, C.E., Wood, C.W., Chaney, P.L., Queiroz, J.F., 2010. Role of aquaculture pond sediments in sequestration of annual global carbon emissions. Environ. Pollut. 158, 2537–2540. https://doi.org/10.1016/j.envpol.2010.04.025

Cole, J.J., Bade, D.L., Bastviken, D., Pace, M.L., Van de Bogert, M., 2010. Multiple approaches to estimating air-water gas exchange in small lakes. Limnol. Oceanogr. Methods 8, 285–293. https://doi.org/10.4319/lom.2010.8.285

Crusius, J., Wanninkhof, R., 2003. Gas transfer velocities measured at low wind speed over a lake. Limnol. Oceanogr. 48, 1010–1017. https://doi.org/10.4319/lo.2003.48.3.1010

Datta, A., Nayak, D.R., Sinhababu, D.P., Adhya, T.K., 2009. Methane and nitrous oxide emissions from an integrated rainfed rice–fish farming system of Eastern India. Agric. Ecosyst. Environ. 129, 228–237. https://doi.org/10.1016/j.agee.2008.09.003

Deemer, B.R., Harrison, J.A., Li, S., Beaulieu, J.J., DelSontro, T., Barros, N., Bezerra-Neto, J.F., Powers, S.M., dos Santos, M.A., Vonk, J.A., 2016. Greenhouse Gas Emissions from Reservoir Water Surfaces: A New Global Synthesis. BioScience 66, 949–964. https://doi.org/10.1093/biosci/biw117

Deemer, B.R., Harrison, J.A., Whitling, E.W., 2011. Microbial dinitrogen and nitrous oxide production in a small eutrophic reservoir: An in situ approach to quantifying hypolimnetic process rates. Limnol. Oceanogr. 56, 1189–1199. https://doi.org/10.4319/lo.2011.56.4.1189

DelSontro, T., Boutet, L., St-Pierre, A., del Giorgio, P.A., Prairie, Y.T., 2016. Methane ebullition and diffusion from northern ponds and lakes regulated by the interaction between temperature and system productivity. Limnol. Oceanogr. 61, S62–S77. https://doi.org/10.1002/lno.10335

Dong, B., Xi, Y., Cui, Y., Peng, S., 2023. Quantifying Methane Emissions from Aquaculture Ponds in China. Environ. Sci. Technol. 57, 1576–1583. https://doi.org/10.1021/acs.est.2c05218

Fang, X., Wang, C., Zhang, T., Zheng, F., Zhao, J., Wu, S., Barthel, M., Six, J., Zou, J., Liu, S., 2022a. Ebullitive CH4 flux and its mitigation potential by aeration in freshwater aquaculture: Measurements and global data synthesis. Agric. Ecosyst. Environ. 335, 108016. https://doi.org/10.1016/j.agee.2022.108016

Fang, X., Zhao, J., Wu, S., Yu, K., Huang, J., Ding, Y., Hu, T., Xiao, S., Liu, S., Zou, J., 2022b. A two-year measurement of methane and nitrous oxide emissions from freshwater aquaculture ponds: Affected by aquaculture species, stocking and water management. Sci. Total Environ. 813, 151863. https://doi.org/10.1016/j.scitotenv.2021.151863

FAO (Ed.), 2018. Meeting the sustainable development goals, The state of world fisheries and aquaculture. Rome.

Flickinger, D.L., Costa, G.A., Dantas, D.P., Proença, D.C., David, F.S., Durborow, R.M., Moraes-Valenti, P., Valenti, W.C., 2020. The budget of carbon in the farming of the Amazon river prawn and tambaqui fish in earthen pond monoculture and integrated multitrophic systems. Aquac. Rep. 17, 100340. https://doi.org/10.1016/j.aqrep.2020.100340

Francová, K., Šumberová, K., Janauer, G.A., Adámek, Z., 2019. Effects of fish farming on macrophytes in temperate carp ponds. Aquac. Int. 27, 413–436. https://doi.org/10.1007/s10499-018-0331-6

Frei, M., Becker, K., 2005. Integrated rice-fish culture: Coupled production saves resources. Nat. Resour. Forum 29, 135–143. https://doi.org/10.1111/j.1477-8947.2005.00122.x

Fuchs, A., Lyautey, E., Montuelle, B., Casper, P., 2016. Effects of increasing temperatures on methane concentrations and methanogenesis during experimental incubation of sediments from oligotrophic and mesotrophic lakes - Fuchs - 2016 - Journal of Geophysical Research: Biogeosciences - Wiley Online Library [WWW Document]. URL https://agupubs.onlinelibrary.wiley.com/doi/full/10.1002/2016JG003328 (accessed 10.22.22).

Gál, D., Pekár, F., Kerepeczki, É., 2016. A survey on the environmental impact of pond aquaculture in Hungary. Aquac. Int. 24, 1543–1554. https://doi.org/10.1007/s10499-016-0034-9

Gebert, J., Köthe, H., Gröngröft, A., 2006. Prognosis of Methane Formation by River Sediments (9 pp). J. Soils Sediments 6, 75–83. https://doi.org/10.1065/jss2006.04.153

Geldhauser, F., Gerstner, P., 2022. Der Teichwirt, scholars-Titel ohne Reihe. Ulmer.

Gorsky, A.L., Racanelli, G.A., Belvin, A.C., Chambers, R.M., 2019. Greenhouse gas flux from stormwater ponds in southeastern Virginia (USA). Anthropocene 28, 100218. https://doi.org/10.1016/j.ancene.2019.100218

Grasset, C., Mendonça, R., Villamor Saucedo, G., Bastviken, D., Roland, F., Sobek, S., 2018. Large but variable methane production in anoxic freshwater sediment upon addition of allochthonous and autochthonous organic matter. Limnol. Oceanogr. 63, 1488–1501. https://doi.org/10.1002/lno.10786

Herzsprung, P., Bozau, E., Büttner, O., Duffek, A., Friese, K., Koschorreck, M., Schultze, M., v. Tümpling jr., W., Wendt-Potthoff, K., 2006. Routine analysis of sediment pore water of high

ionic strength. Acta Hydrochim. Hydrobiol. 34, 593–607. https://doi.org/10.1002/aheh.200500656
Herzsprung, P., Duffek, A., Friese, K., de Rechter, M., Schultze, M., Tümpling, W. v., 2005. Modification of a continuous flow method for analysis of trace amounts of nitrate in iron-rich sediment pore-waters of mine pit lakes. Water Res. 39, 1887–1895. https://doi.org/10.1016/j.watres.2005.02.017
Herzsprung, P., Friese, K., Packroff, G., Schimmele, M., Wendt-Potthoff, K., Winkler, M., 1998. Vertical and annual distribution of ferric and ferrous iron in acidic mining lakes. https://doi.org/10.1002/(SICI)1521-401X(199809)26:5<253::AID-AHEH253>3.0.CO;2-S
Holgerson, M.A., Raymond, P.A., 2016. Large contribution to inland water CO2 and CH4 emissions from very small ponds. Nat. Geosci. 9, 222–226. https://doi.org/10.1038/ngeo2654
Horn, C., Metzler, P., Ullrich, K., Koschorreck, M., Boehrer, B., 2017. Methane storage and ebullition in monimolimnetic waters of polluted mine pit lake Vollert-Sued, Germany. Sci. Total Environ. 584–585, 1–10. https://doi.org/10.1016/j.scitotenv.2017.01.151
Hu, Z., Lee, J.W., Chandran, K., Kim, S., Khanal, S.K., 2012. Nitrous Oxide (N_2O) Emission from Aquaculture: A Review. Environ. Sci. Technol. 46, 6470–6480. https://doi.org/10.1021/es300110x
IPPC, 2021. Summary for policymakers of the scientific review of the impact of climate change on plant pests: A global challenge to prevent and mitigate plant pest risks in agriculture, forestry and ecosystems; Gullino, M.L., Albajes, R., Al-Jboory, I., Angelotti, F., Chakraborty, S., Garrett, K.A., Hurley, B.P., Juroszek, P., Makkouk, K., Pan, X., Stephenson, T., 2021. (Report). Food and Agriculture Organisation of the United Nations. https://doi.org/10.4060/cb4777en
Isidorova, A., Grasset, M., Mendonça, R., Sobek, S., 2019. Methane formation in tropical reservoirs predicted from sediment age and nitrogen | Scientific Reports [WWW Document]. URL https://www.nature.com/articles/s41598-019-47346-7 (accessed 10.22.22).
Joyni, M.J., Kurup, B.M., Avnimelech, Y., 2011. Bioturbation as a possible means for increasing production and improving pond soil characteristics in shrimp-fish brackish water ponds. Aquaculture 318, 464–470. https://doi.org/10.1016/j.aquaculture.2011.05.019
Klaper, H., Kořínek, V., 1992. Eutrophierung und Gewässerschutz | SpringerLink. Gustav-Fischer-Verlag, Jena.
Koschorreck, M., Prairie, Y.T., Kim, J., Marcé, R., 2021. Technical note: CO_2 is not like CH_4 – limits of and corrections to the headspace method to analyse pCO_2 in fresh water. Biogeosciences 18, 1619–1627. https://doi.org/10.5194/bg-18-1619-2021
Kosten, S., Almeida, R.M., Barbosa, I., Mendonça, R., Santos Muzitano, I., Sobreira Oliveira-Junior, E., Vroom, R.J.E., Wang, H.-J., Barros, N., 2020. Better assessments of greenhouse gas emissions from global fish ponds needed to adequately evaluate aquaculture footprint. Sci. Total Environ. 748, 141247. https://doi.org/10.1016/j.scitotenv.2020.141247
Krom, M.D., 1980. Spectrophotometric determination of ammonia: a study of a modified Berthelot reaction using salicylate and dichloroisocyanurate. The Analyst 105, 305. https://doi.org/10.1039/an9800500305
Lazar, J.G., Addy, K., Welsh, M.K., Gold, A.J., Groffman, P.M., 2014. Resurgent Beaver Ponds in the Northeastern United States: Implications for Greenhouse Gas Emissions. J. Environ. Qual. 43, 1844–1852. https://doi.org/10.2134/jeq2014.02.0065
Leal, J.J.F., dos Santos Furtado, A.L., de Assis Esteves, F., Bozelli, R.L., Figueiredo-Barros, M.P., 2007. The role of Campsurus notatus (Ephemeroptera: Polymitarcytidae) bioturbation and sediment quality on potential gas fluxes in a tropical lake. Hydrobiologia 586, 143–154. https://doi.org/10.1007/s10750-006-0570-9
Long, L., Xiao, S.-B., Zhang, C., Zhang, W.-L., Xie, H., Li, Y.-C., Lei, D., Mu, X.-H., Zahng, J.-W., 2016. [Characteristics of Methane Flux Across the Water-air Interface in Subtropical Shallow Ponds]. Huan Jing Ke Xue Huanjing Kexue 37, 4552–4559. https://doi.org/10.13227/j.hjkx.201605093

Lovley, D.R., Phillips, E.J.P., 1987. Competitive Mechanisms for Inhibition of Sulfate Reduction and Methane Production in the Zone of Ferric Iron Reduction in Sediments | Applied and Environmental Microbiology [WWW Document]. URL https://journals.asm.org/doi/full/10.1128/aem.53.11.2636-2641.1987 (accessed 7.26.22).

MacLeod, M.J., Hasan, M.R., Robb, D.H.F., Mamun-Ur-Rashid, M., 2020. Quantifying greenhouse gas emissions from global aquaculture. Sci. Rep. 10, 11679. https://doi.org/10.1038/s41598-020-68231-8

Madigan, M.T., Martinko, J.M., 2006. Brock Mikrobiologie, 11th ed. Pearson Studium, München.

Malyan, S.K., Singh, O., Kumar, A., Anand, G., Singh, R., Singh, S., Yu, Z., Kumar, J., Fagodiya, R.K., Kumar, A., 2022. Greenhouse Gases Trade-Off from Ponds: An Overview of Emission Process and Their Driving Factors. Water 14, 970. https://doi.org/10.3390/w14060970

Mecozzi, M., 1995. Robust regression methods to calibrate a continuous flow analyzer in the colorimetric analysis of inorganic phosphorus in seawater. Talanta 42, 1239–1244. https://doi.org/10.1016/0039-9140(95)01566-T

Meijer, L.E., Avnimelech, Y., 1999. On the use of micro-electrodes in fish pond sediments. Aquac. Eng. 21, 71–83. https://doi.org/10.1016/S0144-8609(99)00024-2

Myhre, G., Samset, B.H., Schulz, M., Balkanski, Y., Bauer, S., Berntsen, T.K., Bian, H., Bellouin, N., Chin, M., Diehl, T., Easter, R.C., Feichter, J., Ghan, S.J., Hauglustaine, D., Iversen, T., Kinne, S., Kirkevåg, A., Lamarque, J.-F., Lin, G., Liu, X., Lund, M.T., Luo, G., Ma, X., van Noije, T., Penner, J.E., Rasch, P.J., Ruiz, A., Seland, Ø., Skeie, R.B., Stier, P., Takemura, T., Tsigaridis, K., Wang, P., Wang, Z., Xu, L., Yu, H., Yu, F., Yoon, J.-H., Zhang, K., Zhang, H., Zhou, C., 2013. Radiative forcing of the direct aerosol effect from AeroCom Phase II simulations. Atmospheric Chem. Phys. 13, 1853–1877. https://doi.org/10.5194/acp-13-1853-2013

Neubauer, S.C., Megonigal, J.P., 2015. Moving Beyond Global Warming Potentials to Quantify the Climatic Role of Ecosystems. Ecosystems 18, 1000–1013. https://doi.org/10.1007/s10021-015-9879-4

Oliveira Junior, E.S., Temmink, R.J.M., Buhler, B.F., Souza, R.M., Resende, N., Spanings, T., Muniz, C.C., Lamers, L.P.M., Kosten, S., 2019. Benthivorous fish bioturbation reduces methane emissions, but increases total greenhouse gas emissions. Freshw. Biol. 64, 197–207. https://doi.org/10.1111/fwb.13209

Ortega, S., Romero González-Quijano, C., Casper, P., Singer, G.A., Gessner, M.O., 2019. Methane emissions from contrasting urban freshwaters: Rates, drivers, and a whole-city footprint. Glob. Change Biol. 25, 4234–4243. https://doi.org/10.1111/gcb.14799

Peacock, M., Audet, J., Jordan, S., Smeds, J., Wallin, M.B., 2019. Greenhouse gas emissions from urban ponds are driven by nutrient status and hydrology. Ecosphere 10, e02643. https://doi.org/10.1002/ecs2.2643

Pechar, L., 2000. Impacts of long-term changes in fishery management on the trophic level water quality in Czech fish ponds. Fish. Manag. Ecol. 7, 23–31. https://doi.org/10.1046/j.1365-2400.2000.00193.x

Phan-Van, M., Rousseau, D., De Pauw, N., 2008. Effects of fish bioturbation on the vertical distribution of water temperature and dissolved oxygen in a fish culture-integrated waste stabilization pond system in Vietnam. Aquaculture 281, 28–33. https://doi.org/10.1016/j.aquaculture.2008.04.033

Potužák, J., Hůda, J., Pechar, L., 2007. Changes in fish production effectivity in eutrophic fishponds—impact of zooplankton structure. Aquac. Int. 15, 201–210. https://doi.org/10.1007/s10499-007-9085-2

R Core Team, 2019. R Development Core Team. R: A language and environment for statistical computing (R Foundation for Statistical Computing, 2021).

Redfield, A.C., 1958. The biological control of chemical factors in the environment. Am. J. Sci. 46, 205–221.

Říha, M., Rabaneda-Bueno, R., Jarić, I., Souza, A., Vejřík, L., Draštík, V., Blabolil, P., Holubová, M., Jůza, T., Gjelland, K.Ø., Rychtecký, P., Sajdlová, Z., Kočvara, L., Tušer, M., Prchalová, M., Seďa, J., Peterka, J., 2021. Dynamics of the habitat use of three predatory freshwater fish in a lentic ecosystem | bioRxiv [WWW Document]. URL https://www.biorxiv.org/content/10.1101/2021.12.16.471647v1.abstract (accessed 10.23.22).

Rõõm, E.-I., Nõges, P., Feldmann, T., Tuvikene, L., Kisand, A., Teearu, H., Nõges, T., 2014. Years are not brothers: Two-year comparison of greenhouse gas fluxes in large shallow Lake Võrtsjärv, Estonia. J. Hydrol. 519, 1594–1606. https://doi.org/10.1016/j.jhydrol.2014.09.011

Rosentreter, J.A., Borges, A.V., Deemer, B.R., Holgerson, M.A., Liu, S., Song, C., Melack, J., Raymond, P.A., Duarte, C.M., Allen, G.H., Olefeldt, D., Poulter, B., Battin, T.I., Eyre, B.D., 2021. Half of global methane emissions come from highly variable aquatic ecosystem sources. Nat. Geosci. 14, 225–230. https://doi.org/10.1038/s41561-021-00715-2

Rutegwa, M., Gebauer, R., Veselý, L., Regenda, J., Strunecký, O., Hejzlar, J., Drozd, B., 2019. Diffusive methane emissions from temperate semi-intensive carp ponds. Aquac. Environ. Interact. 11, 19–30. https://doi.org/10.3354/aei00296

Schlesinger, W.H., 2009. On the fate of anthropogenic nitrogen | PNAS [WWW Document]. URL https://www.pnas.org/doi/full/10.1073/pnas.0810193105 (accessed 7.28.22).

Schwoerbel, J., Brendelberger, H., 2016. Einführung in die Limnologie: Stoffhaushalt - Lebensgemeinschaften - Technologie. Springer, Berlin, Heidelberg. https://doi.org/10.1007/978-3-662-63334-2

Seitzinger, S.P., Kroeze, C., Styles, R.V., 2000. Global distribution of N2O emissions from aquatic systems: natural emissions and anthropogenic effects. Chemosphere - Glob. Change Sci., Atmospheric Nitrous Oxide 2, 267–279. https://doi.org/10.1016/S1465-9972(00)00015-5

Selvam, B.P., Natchimuthu, S., Arunachalam, L., Bastviken, D., 2014. Methane and carbon dioxide emissions from inland waters in India – implications for large scale greenhouse gas balances. Glob. Change Biol. 20, 3397–3407. https://doi.org/10.1111/gcb.12575

Shaher, S., Chanda, A., Das, S., Das, I., Giri, S., Samanta, S., Hazra, S., Mukherjee, A.D., 2020. Summer methane emissions from sewage water–fed tropical shallow aquaculture ponds characterized by different water depths. Environ. Sci. Pollut. Res. 27, 18182–18195. https://doi.org/10.1007/s11356-020-08296-0

Soued, C., del Giorgio, P.A., Maranger, R., 2016. Nitrous oxide sinks and emissions in boreal aquatic networks in Québec. Nat. Geosci. 9, 116–120. https://doi.org/10.1038/ngeo2611

Teodoru, C.R., Bastien, J., Bonneville, M.-C., del Giorgio, P.A., Demarty, M., Garneau, M., Hélie, J.-F., Pelletier, L., Prairie, Y.T., Roulet, N.T., Strachan, I.B., Tremblay, A., 2012. The net carbon footprint of a newly created boreal hydroelectric reservoir. Glob. Biogeochem. Cycles 26. https://doi.org/10.1029/2011GB004187

Tong, C., Bastviken, D., Tang, K.W., Yang, P., Yang, H., Zhang, Y., Guo, Q., Lai, D.Y., 2021. Annual CO2 and CH4 fluxes in coastal earthen ponds with Litopenaeus vannamei in southeastern China. Aquaculture 545, 737229.

van Bergen, T.J.H.M., Barros, N., Mendonça, R., Aben, R.C.H., Althuizen, I.H.J., Huszar, V., Lamers, L.P.M., Lürling, M., Roland, F., Kosten, S., 2019. Seasonal and diel variation in greenhouse gas emissions from an urban pond and its major drivers. Limnol. Oceanogr. 64, 2129–2139. https://doi.org/10.1002/lno.11173

Verdegem, M.C.J., Bosma, R.H., 2009. Water withdrawal for brackish and inland aquaculture, and options to produce more fish in ponds with present water use. Water Policy 11, 52–68. https://doi.org/10.2166/wp.2009.003

Wanninkhof, R., 1992. Relationship between wind speed and gas exchange over the ocean. J. Geophys. Res. Oceans 97, 7373–7382. https://doi.org/10.1029/92JC00188

Webb, J.R., Hayes, N.M., Simpson, G.L., Leavitt, P.R., Baulch, H.M., Finlay, K., 2019. Widespread nitrous oxide undersaturation in farm waterbodies creates an unexpected greenhouse gas sink. Proc. Natl. Acad. Sci. 116, 9814–9819. https://doi.org/10.1073/pnas.1820389116

West, W., Coloso, J., Jones, S., 2012. Effects of algal and terrestrial carbon on methane production rates and methanogen community structure in a temperate lake sediment - WEST - 2012 -

Freshwater Biology - Wiley Online Library [WWW Document]. URL https://onlinelibrary.wiley.com/doi/abs/10.1111/j.1365-2427.2012.02755.x?casa_token=b130kokJQw8AAAAA:x6ulsVRu080potV-zRqj_tuVi8d1MC0F6DJp25enpoFBLsyg9vB0DzFN1AtL6mZlRPQhtr_knWkSOswZ (accessed 10.22.22).

Wik, M., Thornton, B.F., Bastviken, D., Uhlbäck, J., Crill, P.M., 2016. Biased sampling of methane release from northern lakes: A problem for extrapolation. Geophys. Res. Lett. 43, 1256–1262. https://doi.org/10.1002/2015GL066501

Winslow, L., Zwart, J., Batt, R., Dugan, H., Woolway, R., Corman, J., Hanson, P., Read, J., 2016. LakeMetabolizer: an R package for estimating lake metabolism from free-water oxygen using diverse statistical models. Inland Waters 6, 622–636. https://doi.org/10.1080/IW-6.4.883

Yang, P., Zhang, Y., Yang, H., Guo, Q., Lai, D.Y.F., Zhao, G., Li, L., Tong, C., 2020. Ebullition was a major pathway of methane emissions from the aquaculture ponds in southeast China. Water Res. 184, 116176. https://doi.org/10.1016/j.watres.2020.116176

Yuan, J., Liu, D., Xiang, J., He, T., Kang, H., Ding, W., 2021. Methane and nitrous oxide have separated production zones and distinct emission pathways in freshwater aquaculture ponds. Water Res. 190, 116739. https://doi.org/10.1016/j.watres.2020.116739

Yuan, J., Xiang, J., Liu, D., Kang, H., He, T., Kim, S., Lin, Y., Freeman, C., Ding, W., 2019. Rapid growth in greenhouse gas emissions from the adoption of industrial-scale aquaculture. Nat. Clim. Change 9, 318–322. https://doi.org/10.1038/s41558-019-0425-9

Zhang, D., Tian, X., Dong, S., Chen, Y., Feng, J., He, R.-P., Zhang, K., 2020. Carbon budgets of two typical polyculture pond systems in coastal China and their potential roles in the global carbon cycle. Aquac. Environ. Interact. 12, 105–115. https://doi.org/10.3354/aei00349

Zhang, Y., Tang, K.W., Yang, P., Yang, H., Tong, C., Song, C., Tan, L., Zhao, G., Zhou, X., Sun, D., 2022. Assessing carbon greenhouse gas emissions from aquaculture in China based on aquaculture system types, species, environmental conditions and management practices. Agric. Ecosyst. Environ. 338, 108110. https://doi.org/10.1016/j.agee.2022.108110

Zhao, J., Zhang, M., Xiao, W., Jia, L., Zhang, X., Wang, J., Zhang, Z., Xie, Y., Pu, Y., Liu, S., Feng, Z., Lee, X., 2021. Large methane emission from freshwater aquaculture ponds revealed by long-term eddy covariance observation. Agric. For. Meteorol. 308–309. https://doi.org/10.1016/j.agrformet.2021.108600

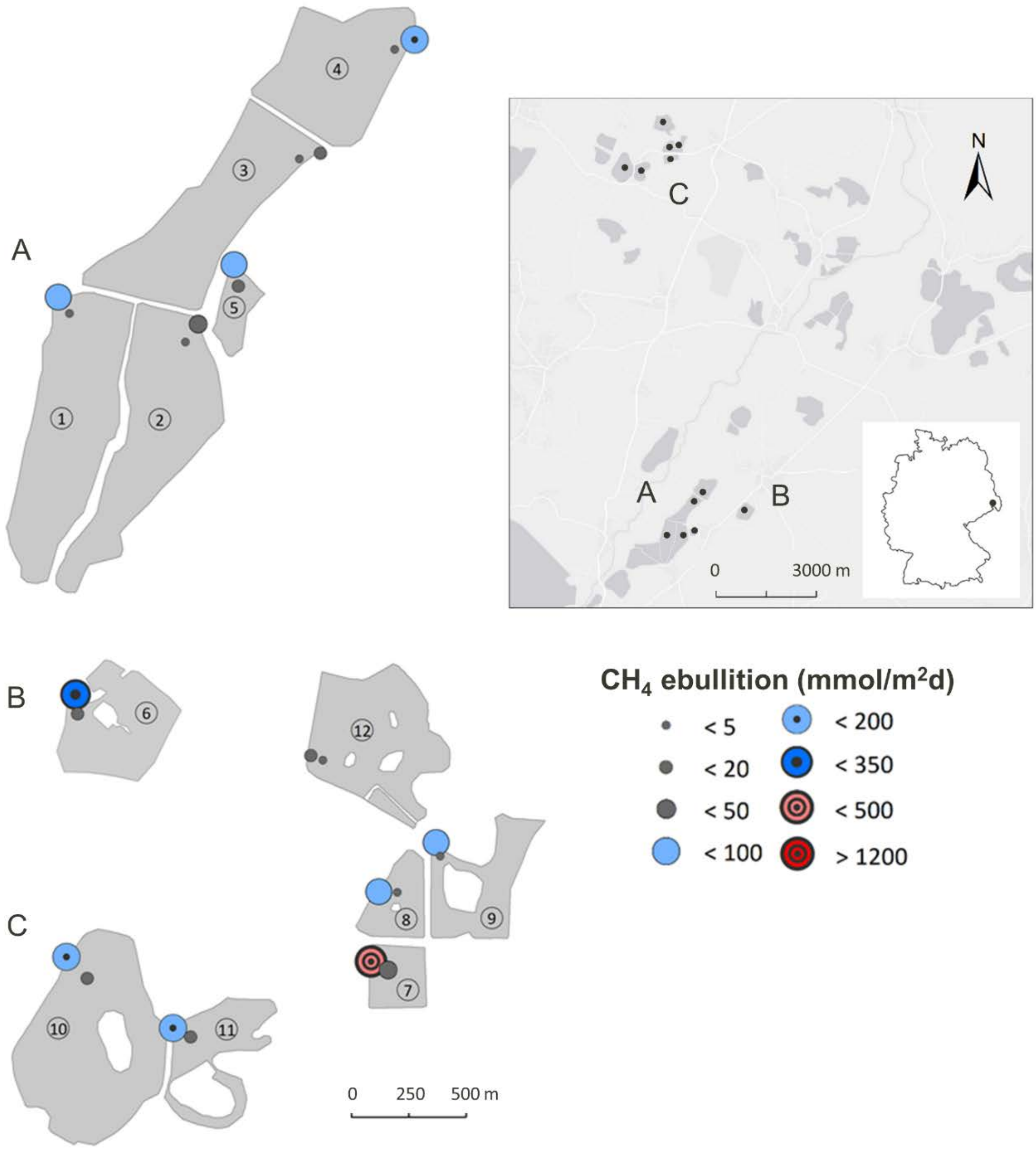

Figure 1: CH_4 ebullition during the survey of 12 extensively to semi-intensively managed fish ponds close to Bautzen, Germany, in June 2021 (bubble traps over 24h or 48h). Investigated temperate freshwater fish ponds sorted according to companies and spatial distribution: A: 1) Teich 1, 2) Teich 2, 3) Teich 3, 4) Teich 4, 5) Brauereiteich; B: 6) Straßenteich; C: 7) Gerstenteich, 8) Kl. Krähenteich, 9) Al. Krähenteich, 10) Inselteich, 11) Thronteich, 12) Heikteich (nursery carp pond).

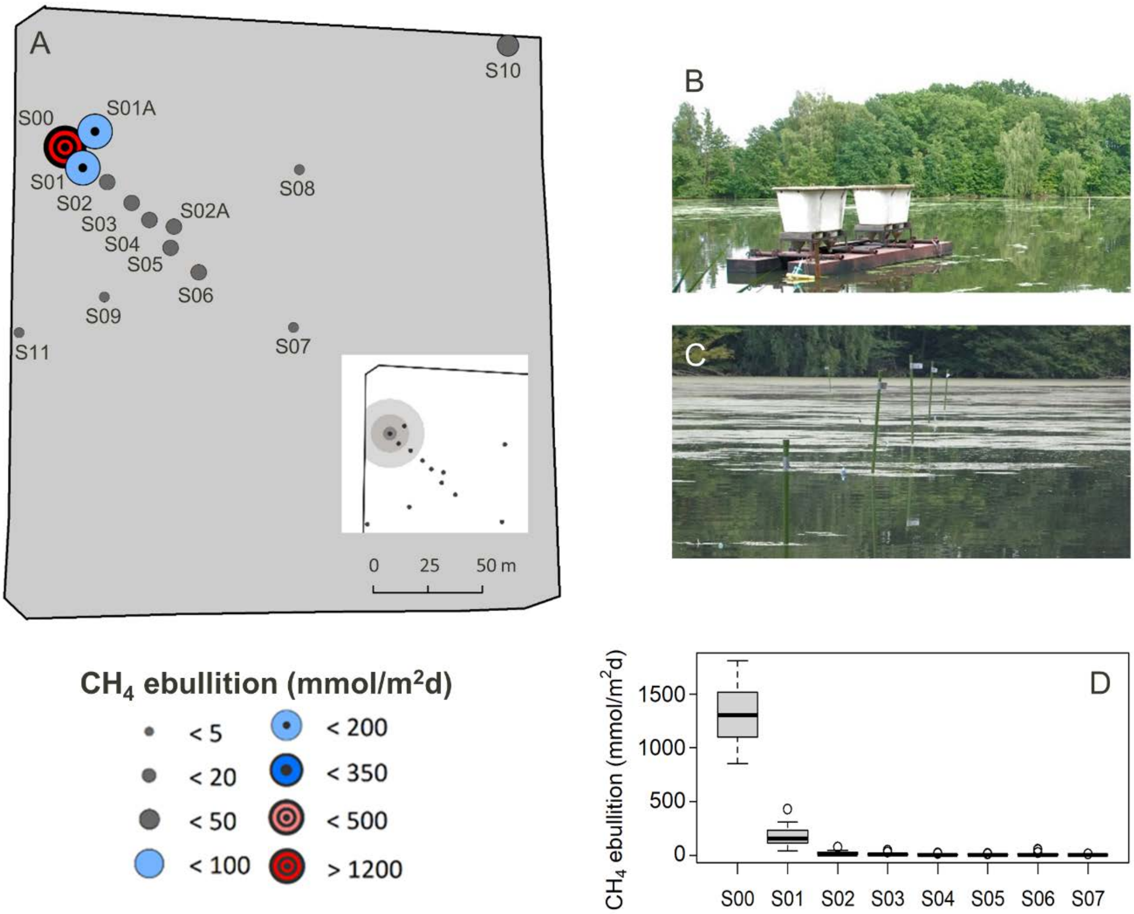

Figure 2: CH_4 ebullition during the detailed Gerstenteich-study in Sept. 2021: (A) Mean CH_4 ebullition over 48h (S00 – S11) or 24h (S01A and S02A). CH_4 ebullition scheme with hotspot at the pellet feeder (S00), transition areas and the background. (B) Photo of the automatic pellet feeder and (C) the transect. (D) Decrease of CH_4 ebullition with distance from the feeding site (boxplot with median (black line), 25% and 75% quantiles (box), outliers of 1.5 IQR (whiskers) and extreme outliers (circles)). Exponential fit: $y = 1301.18 \exp(-x/3.52) + 2.27$ with R^2 0.99.

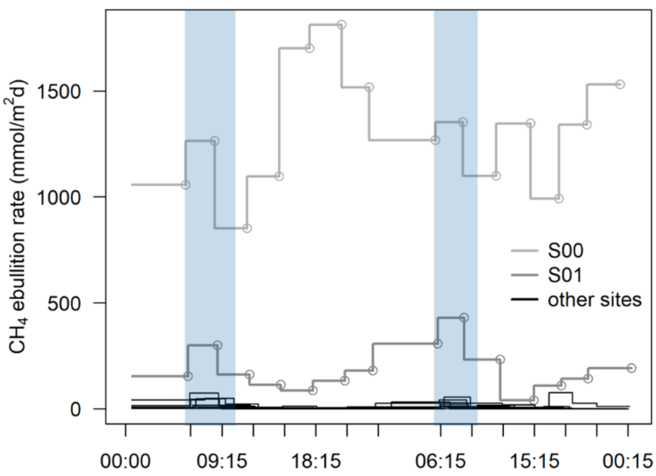

Figure 3: Temporal variability of CH_4 ebullition rate during the detailed Gerstenteich-study in Sept. 2021. Mean sampling times are indicated as circles for S00 and S01. Periods with increased ebullition shaded.

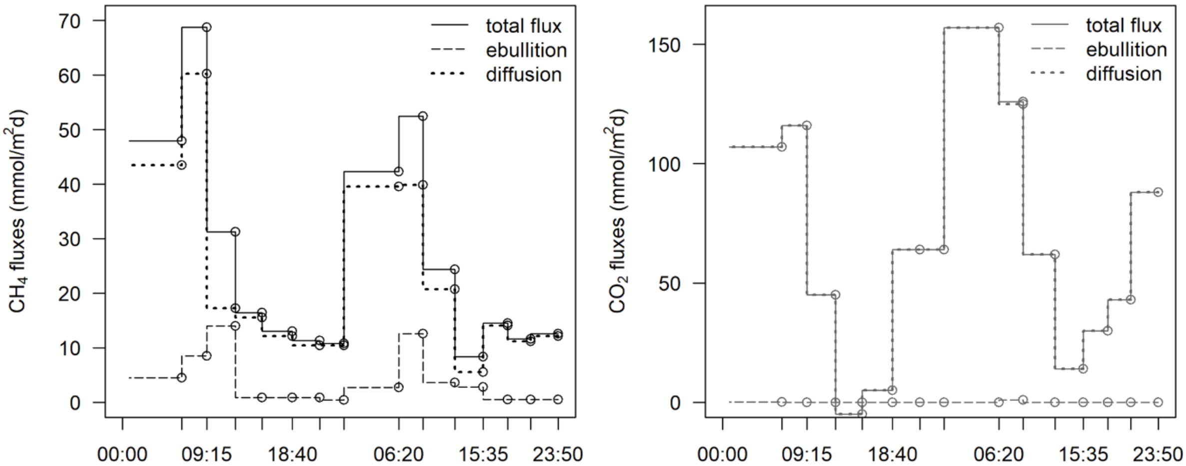

Figure 4: Diurnal course of CH_4 and CO_2 ebullition and diffusion at site S05 of the detailed Gerstenteich-study in Sept. 2021. Sampling (circles) at this site started at 6:30 a.m. and lasted until midnight. Total fluxes as the sum of ebullition and diffusion.